International Society for Rock Mechanics and Rock Engineering
Norwegian Group for Rock Mechanics

ISRM International Symposium
Eurock 2025 – Expanding the Underground Space
Trondheim, Norway, 16-20 June
ISBN 978-82-8208-079-8

Numerical analysis of the mechanical stability of salt caverns for Underground Hydrogen Storage under cyclic Solicitations

H. Djizanne
Ineris, Verneuil-en-Halatte, France
hippolyte.djizanne@ineris.fr

B. Brouard
Brouard Consulting, Paris, France

Abstract

Hydrogen has emerged as a critical energy vector in the transition towards clean and renewable energy systems, providing a viable alternative to fossil fuels. Underground Hydrogen Storage (UHS) in salt caverns, created through solution mining, is currently the most promising large-scale storage method due to the very low permeability of rock salt and its mechanical stability. However, the safety and integrity of salt caverns remain key challenges under severe operating conditions, particularly fast cyclic loading (repeated gas injection and withdrawal) and rapid depressurization. These processes cause time-dependent deformation (creep closure) of the cavern, and rapid pressure drops result in gas cooling, generating thermal stresses that can trigger tensile fracturing at the cavern wall and roof. This study investigates the mechanical behaviour of salt caverns under cyclic solicitations using advanced numerical modelling implemented in the LOCAS software. The non-linear and time-dependent response of rock salt is analysed by incorporating the Munson-Dawson creep law, and a dilatancy criterion to assess damage progression. Key findings include the progressive creep closure of caverns, with accelerated deformation near the cavern wall, and the redistribution of stresses leading to significant orthoradial contraction and radial expansion. Thermal diffusion, exacerbated by hydrogen low thermal capacity, further amplifies mechanical stresses. A Factor of Safety (FoS) analysis using the Spiers and DeVries criteria confirms that no dilation zone ($0 < FoS < 1$) develops after 7-year of seasonal cyclic loading, ensuring cavern stability under the analysed conditions. The study highlights the cumulative effects of cyclic loading on stress, strain, and displacement distributions, offering practical recommendations for optimizing operational parameters, such as pressure cycling and thermal, gas velocity and interface monitoring, to maintain the long-term stability and safety of salt caverns for hydrogen storage.

Keywords

UHS, salt caverns, mechanical stability, numerical modelling, cyclic loading.

1 Introduction

The global energy transition is driving the development of clean and renewable energy sources to reduce greenhouse gas emissions and mitigate climate change. In this context, hydrogen has emerged

as a versatile and promising energy vector due to its ability to replace fossil fuels in industrial, transportation, and energy storage applications. One of the main challenges for hydrogen deployment at scale is the need for safe, efficient, and cost-effective storage solutions to balance supply and demand. Among the available options, Underground Hydrogen Storage (UHS) in salt caverns stands out as the most viable method for large-scale storage.

Salt caverns, created through solution mining, provide a unique environment for gas storage. Their key advantages include very low permeability to gases, good geomechanical stability, and the ability to accommodate high pressures. Salt caverns have been successfully utilized for natural gas storage, but also for hydrogen storage, with notable examples in the UK and USA. In the UK, brine compensation technique is used to optimize storage operations, enabling the withdrawal and injection of gas without the need for cushion gas, which reduces operational costs. Despite these advantages, UHS in salt caverns introduces several technical challenges related to their mechanical and thermal responses under severe operating conditions.

One of the primary concerns for UHS is the impact of cyclic loading, resulting from repeated gas injection and withdrawal phases. Cyclic loading induces time-dependent deformation or creep closure of the cavern due to the elasto-viscoplastic behavior of rock salt. Over time, this process can lead to significant cavern convergence, reducing storage capacity and potentially compromising operational safety. Additionally, rapid depressurization during gas withdrawal causes hydrogen cooling, where gas temperature drops sharply depending on withdrawal rates and cavern geometry. This cooling generates thermal stresses at the cavern walls and roof, which may lead to tensile fracturing, compromising cavern integrity (Bérest et al. 2007, Djizanne et al. 2023). These combined thermal and mechanical effects pose challenges in predicting the long-term stability and performance of salt caverns for hydrogen storage.

To address these challenges, advanced numerical modelling techniques are essential for evaluating the coupled thermo-mechanical behaviour of salt caverns under cyclic solicitations. Such models must incorporate the non-linear, time-dependent deformation mechanisms of rock salt, including dislocation creep, pressure solution creep, and dilatancy, which describe the progression of damage in the salt formation. The LOCAS software integrates these constitutive models, enabling detailed simulations of stress distribution, strain evolution, thermal diffusion, and damage development around the cavern walls. This paper focuses on the mechanical stability of salt caverns used for UHS under cyclic loading and rapid depressurization conditions. Key objectives of this work include:

1. Evaluating the evolution of cavern temperature during cyclic operations.
2. Analysing the redistribution of stresses and strains near the cavern wall.
3. Quantifying creep-induced volume closure and displacement.
4. Assessing the risk of damage initiation through Factor of Safety (FoS) analysis using established failure criteria (Spiers et al. 1988, DeVries et al. 2005).

By providing insights into the coupled thermo-mechanical of rock salt, this study aims to improve the design and operational strategies for hydrogen storage in salt caverns. The results are expected to contribute to the development of safe and efficient storage systems that support the increasing demand for hydrogen as part of the global energy transition. The remainder of this paper is organized as follows: Section 2 presents the model definition, including the cavern geometry, material properties, and loading conditions while Section 3 discusses the numerical results, including cavern convergence, stress and strain distributions, displacement fields, evaluates the Factor of Safety and identifies critical zones.

2 Model definition

2.1 Description of the studied cavern

A single cavern at an average depth of 1,373 m is considered; this cavern is vertical, and its volume is 335,074 m^3. The cavern height is 223 m and its average diameter is 65 m.

2.2 Thermomechanical model

The temperature at ground level is assumed to be 10°C. The geothermal gradient is 4.36°C/100 m in the overburden and 1.6°C/100 m in the salt formation. On the lateral surface of the model, the

geostatic stress is fixed (see densities in Table 1 in Appendix; $g = 9.81$ m/s^2 is assumed). Vertical displacements are null at the bottom of the model.

2.2.1 Elasticity

The density and elastic properties considered for overburden and rock salt are given in Table 1. Thermo-elasticity of rock salt must be considered in the computation as large gas-temperature variations can be expected at the cavern wall during the blowout. The thermo-elastic strain writes:

$$\varepsilon_{th} = \alpha_{salt}\left(T - T_0\right) \tag{1}$$

where α_{salt} is the coefficient of thermal expansion of rock salt and T_0 is a reference temperature. A value of $\alpha_{salt} = 4\times10^{-5}$ /K is considered.

Table 1. Considered densities, elastic and thermal properties.

Rock	Density	Elastic parameters		Thermal properties		
		E (GPa)	ν (-)	K (W/m-K)	k (x 10^{-6} m^2/s)	C_p (J/kg-K)
Overburden	2,520	8.6	0.23	3		
Salt	2,200	25.0	0.25	6.07	3	920

Where K is the thermal conductivity, k is the thermal diffusivity and C_p is the specific heat.

2.2.2 Salt creep

The Munson-Dawson model (Munson and Dawson, 1982) comprises two differential equations: the strain-rate equations that give the viscoplastic strain rates; and the evolutionary equation that gives the rate of change of an internal variable describing the transient creep rate. A simplified version of Munson-Dawson law can then be written as follows:

$$\dot{\varepsilon}_{ij}^{vp} = \frac{\partial\sigma}{\partial\sigma_{ij}} F\dot{\varepsilon}_{ss} \qquad \begin{cases} F = e^{\Delta\left(1-\varsigma/\varepsilon_t^*\right)^2} & \text{when } \varsigma \le \varepsilon_t^* \\ F = e^{-\delta\left(1-\varsigma/\varepsilon_t^*\right)^2} & \text{when } \varsigma \ge \varepsilon_t^* \end{cases} \tag{2}$$

$$\dot{\varsigma} = \left(F-1\right)\dot{\varepsilon}_{ss} \qquad \dot{\varepsilon}_{ss} = A\exp\left(-Q/RT\right)\sigma^n \tag{3}$$

$$\sigma = \sqrt{3J_2} \qquad J_2 = \frac{1}{2}s_{ij}s_{ij} \qquad \varepsilon_t^* = K_0 e^{cT}\left(\sigma/\mu\right)^m \tag{4}$$

$$\mu = E/2\left(1+\nu\right) \text{ and } \Delta = \alpha_{\mathrm{w}} + \beta_w Log_{10}\left(\sigma/\mu\right) \tag{5}$$

This simplified version of the law has 9 parameters: $A, n, Q/R, m, K_0, \alpha_w, \beta_w, \delta$ and c. The proposed set of parameters for this creep law are given in Table 2. Note that, for simplicity, reverse creep is not considered in the model. As a variant, $A = 6.4$ MPa$^{-3.1}$yr^{-1} is considered to discuss the case of a fast-creeping salt.

Table 2. Sets of parameters for Munson-Dawson creep law.

Parameter	SI Units	
	Unit	Value
A	MPa^{-n}·year^{-1}	0.74
n	-	5
Q/R	K	5,032
K_0	/MPa m	7 ×10-7
m	-	3
c	K^{-1}	0.00902
α_w	-	-13.2
β_w	-	-7.738
δ	-	0.58

2.3 Cyclic loading

The selected salt cavern is subjected to cycles of injection and withdrawal of pure gaseous hydrogen supposed to be injected at 40°C. One cycle consists of a continuous withdrawal for 60 days, followed

by 60 days of stand-by, then a continuous injection for 5 days, also followed by 100 days of stand-by. Figure 1 shows the evolution of cavern pressure (grey) and temperature (hydrogen in red, brine in blue) over time under cyclic loading. The cavern pressure fluctuates sharply between 60 barg and 217.2 barg during injection and withdrawal phases, staying below the maximum allowable pressure (P_{max} = 227 barg). Correspondingly, the hydrogen temperature (red) drops significantly during pressure reduction, reaching below 30°C due to hydrogen expansion, and rises during injection, exceeding the geothermal temperature (green dashed line). The brine temperature (orange) exhibits a more stable trend with minor fluctuations, reflecting its slower thermal response. It is worth mentioning that the cavern volume is 96.7 % filled with hydrogen, the residual brine fills the rest of the 3.3% with a brine/gas interface located 9.4 m over 223 m from the cavern bottom. The repeated cooling cycles of hydrogen indicate significant thermal stress on the cavern walls, which may lead to mechanical damage.

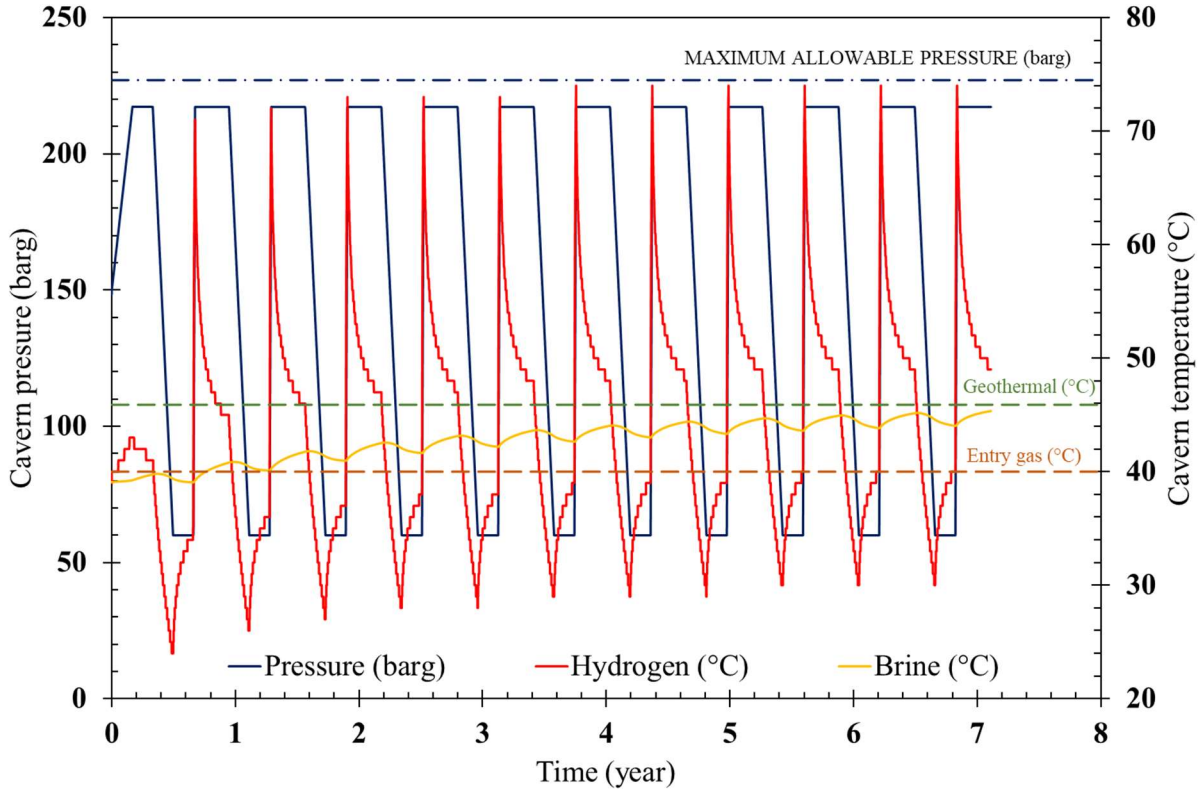

Fig. 1 Evolution of cavern pressure and temperature.

Fig. 2 and 3 compare temperature distributions in rock salt at the end of debrining and end of cyclic loading. Cyclic loading causes significant thermal diffusion, with cooler zones (green to blue) near the cavern wall extending deeper into the formation. Fig. 2 confirms this, where temperature near the cavern wall drops to around 41°C after debrining (blue) and stabilizes near 43°C after cyclic loading (red), while temperatures further from the cavern remain near the undisturbed geothermal gradient.

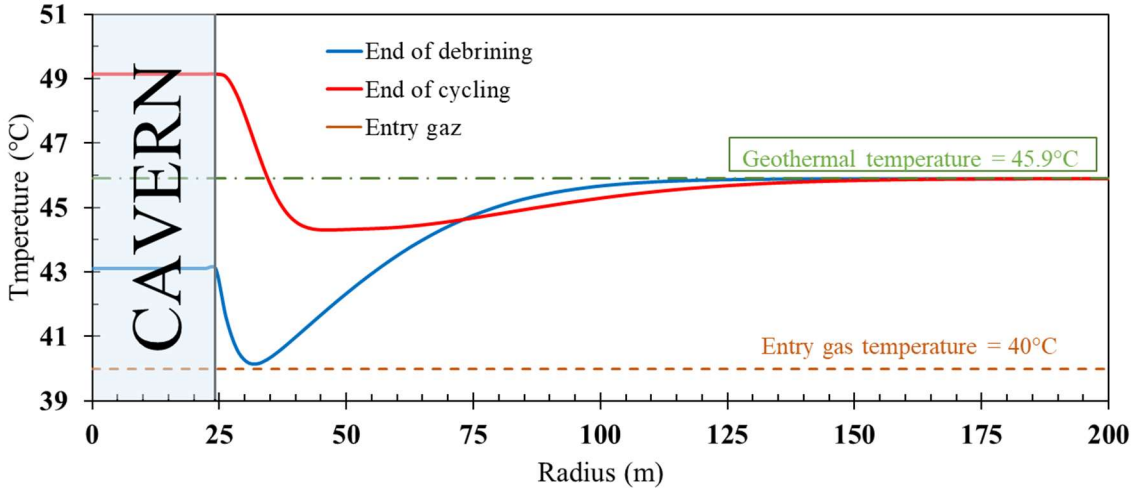

Fig. 2 Radial distribution of temperature a cavern mid-depth (1,373 m).

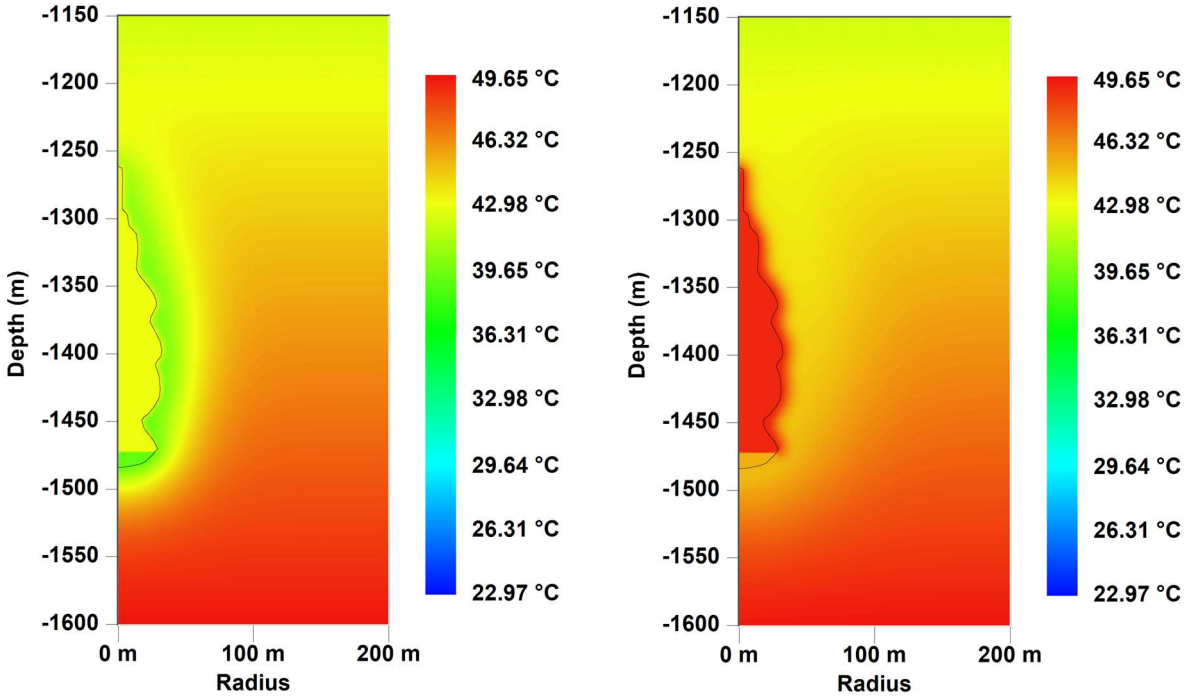

Fig. 3 Contours plot of the temperature at the end of debrining and at the end of cyclic loading.

3 Modelling result

3.1 Cavern creep closure

Fig. 4 shows the percentage variation of cavern volume over time under cyclic loading, illustrating progressive creep closure. The step-like pattern indicates that each loading cycle (e.g., pressure reductions) accelerates deformation, while short plateaus suggest periods of relative stability. Initial closure is rapid (~4% in the first year) due to stress redistribution, followed by a slower but consistent trend, reaching ~14% volume loss after 7 years. This highlights the elasto-viscoplastic behaviour of the surrounding rock salt, where cyclic loading exacerbates time-dependent deformation.

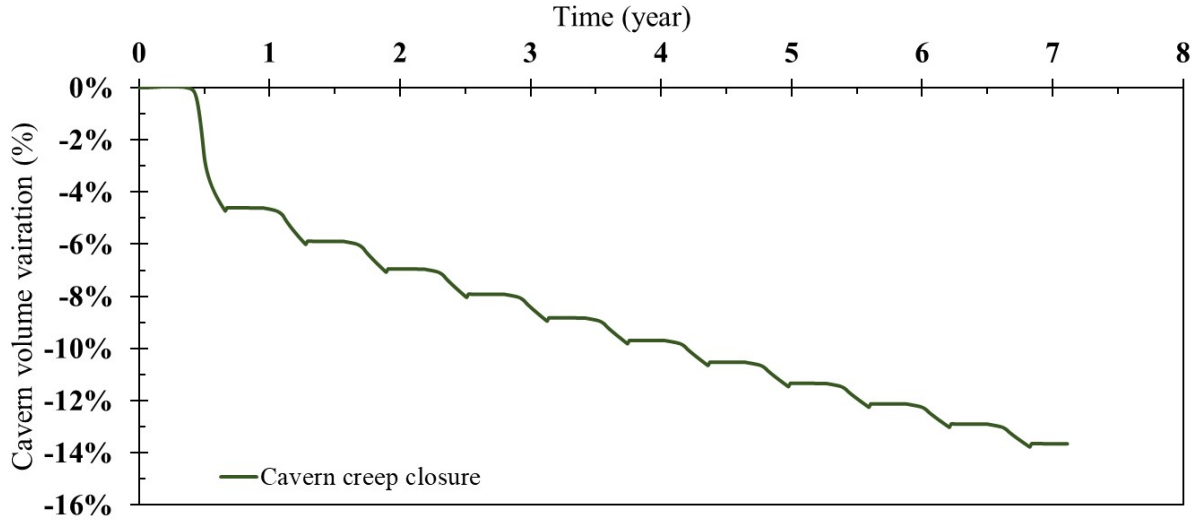

Fig. 4. Cavern volume variation during cyclic loading.

3.2 Stresses distribution

The stress distribution (radial, orthoradial, and vertical stresses) as a function of radius at the cavern mid-depth (1373 m) are compared to the geostatic pressure (dashed line) on Figure 5. At the vicinity of the cavern wall which is the critical zone for potential damage or fracture initiation, all three stresses deviate significantly from geostatic equilibrium due to stress concentration, with the orthoradial stress (σ_{tt}, red) exhibiting the largest compressive drop, indicating localized stress redistribution. The radial stress (σ_{rr}, blue) starts at a lower compressive value and increases gradually with distance, while the vertical stress (σ_{zz}, green) shows intermediate behaviour. Beyond

approximately 50 m, all stresses progressively stabilize and converge toward geostatic pressure, reflecting the dissipation of stress perturbations away from the cavern boundary.

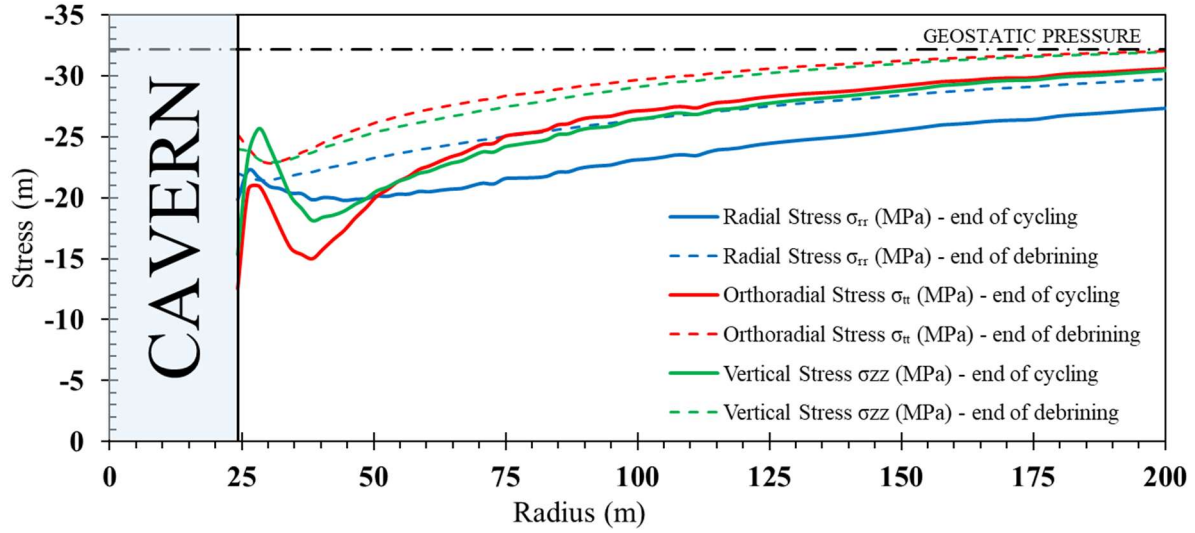

Fig. 5 Distribution of stresses (σ_{rr}, σ_{tt} and σ_{zz}) at cavern mid-depth (1,373 m).

A comparison of effective stress distribution at the end of debrining and at end of cyclic loading, shows a clear expansion of tensile effective zones (magenta regions on Fig. 6) along the cavern wall under cyclic loading. While tensile stresses initially remain localized at specific zone at cavern wall, cyclic loading significantly redistributes stress, intensifying tensile regions and propagating them deeper into the salt formation. This stress amplification near the cavern wall highlights the increased risk of fracture initiation and structural instability (Bérest et al. 2007).

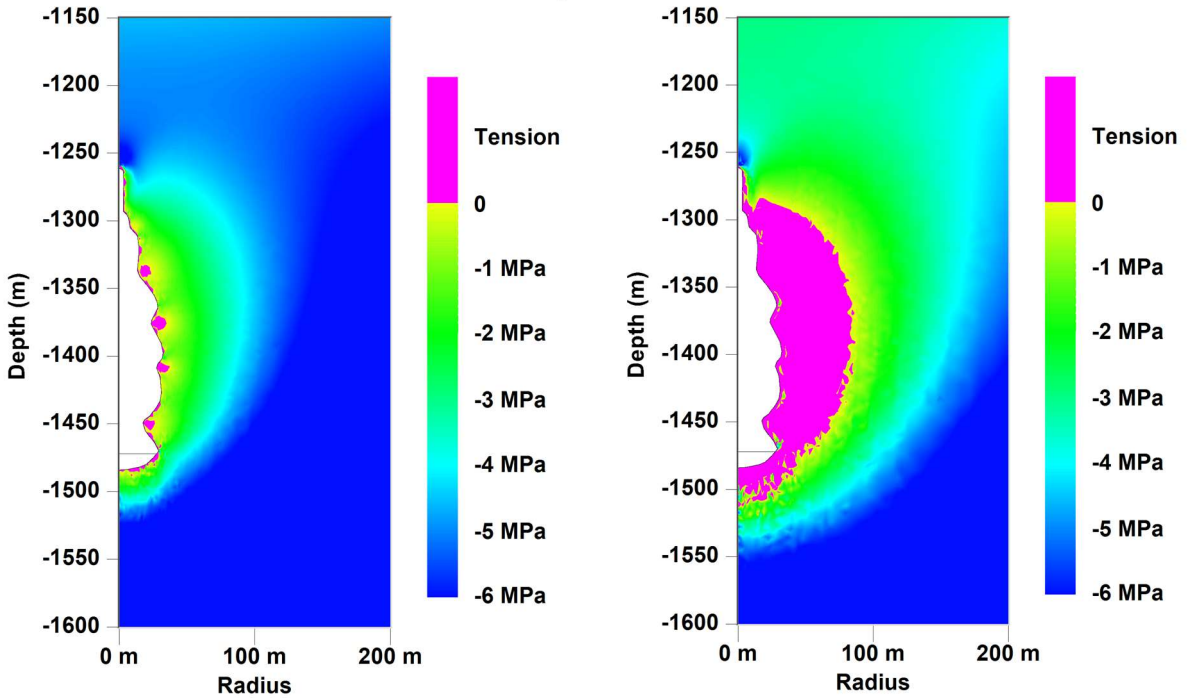

Fig. 6 Effective stress at the end of debrining (left) and at the end of cyclic loading (right).

3.3 Strains and displacements

Strain redistribution reflects the extend of the disturbed area from the salt cavern wall. Fig. 7 shows the strain distribution at the cavern mid-depth (1,373 m), comparing results at the end of debrining (dashed lines) and at the end of cyclic loading (solid lines). The radial strain (ε_{rr}, blue) is positive, indicating expansion due to stress relief, and it is more pronounced at the end of cyclic loading compared to debrining. Conversely, orthoradial strain (ε_{tt}, red) shows significant contraction close to the cavern wall, reaching nearly -8% with cyclic loading intensifying the strain compared to debrining, reflecting more compressive tangential strain with cumulated cyclic loads. The vertical strain (ε_{zz}, green) transitions from slight dilatation near the wall to moderate contraction before stabilization further into the rock mass. Beyond approximately 50 m, all strains components stabilize, approaching zero as the disturbance diminishes. Cyclic loading intensifies strain anisotropy near the cavern wall,

with radial expansion and orthoradial contraction being the dominant deformation mechanisms. The cumulative effect of cyclic loading induces cavern convergence and displacement. Fig. 8. compare radial and vertical displacement at the end of cyclic loading. At the end of debrining, radial and vertical displacement are limited and concentrated near the cavern wall, indicating minor strain. After cyclic loading, the radial displacement significantly increases, with a pronounced gradient extending deeper into the surrounding rock salt, reaching over -2,239 mm in the lower part of the cavern. The expanded zone of deformation (green to blue) reflects creep-induced closure and stress redistribution due to cyclic pressure changes. After cyclic loading, significant vertical displacement develops near the cavern wall and roof, with values exceeding -741 mm (blue zones), indicating subsidence and downward deformation. The increased displacement near the cavern wall highlights the cumulative effect of cyclic loading in intensifying vertical creep and subsidence that may compromise cavern integrity and surface stability over time.

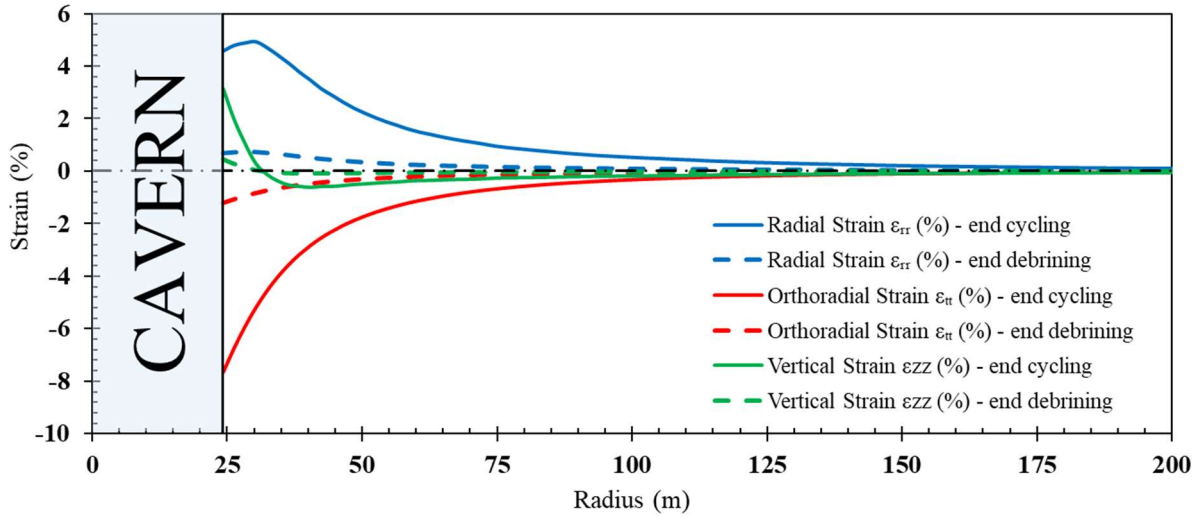

Fig. 7 Strains distribution (ε_{rr}, ε_{tt} and ε_{zz}) at cavern mid-depth (1,373 m).

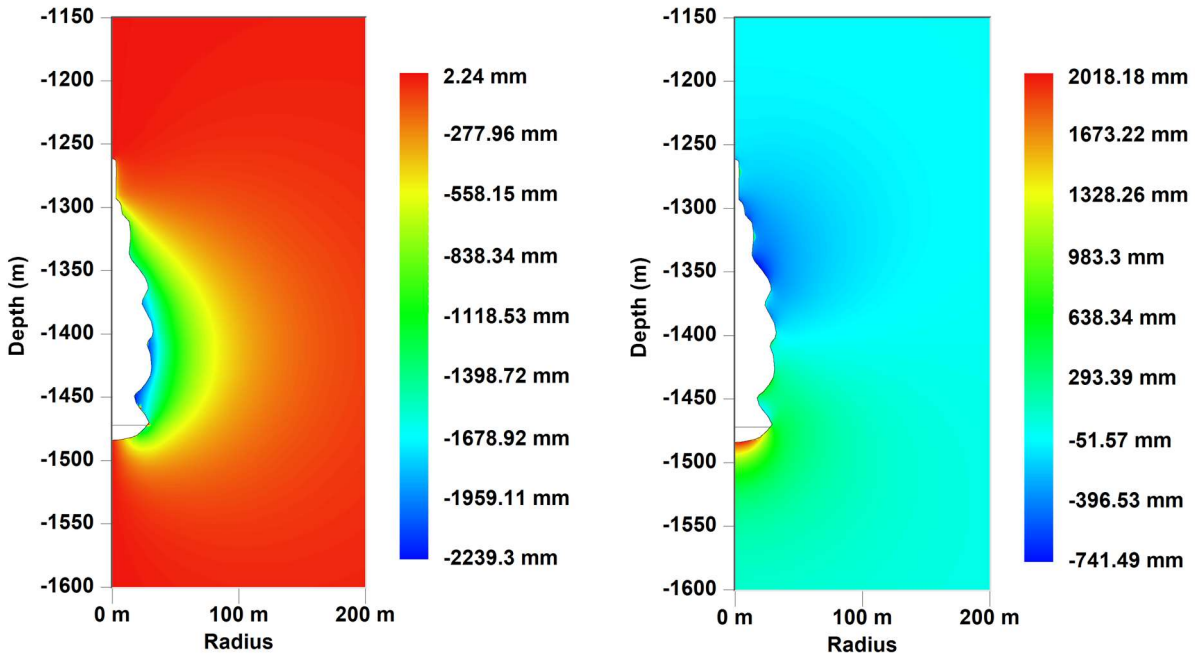

Fig. 8. Radial (left) and vertical (right) displacement at the end of cyclic loading.

3.4 Factor of safety (FoS)

Figure 11 presents contour plots of the Factor of Safety (FoS) at the end of cyclic loading, using the Spiers criterion (left) from Spiers et al. 1988 and the DeVries criterion (right) from DeVries et al. 2005. Overall, the absence of a dilation zone in both criteria confirms that the salt cavern remains structurally stable under the applied cyclic loading, with the DeVries criterion offering a more sensitive assessment of stress variations near the cavern wall compared to the more conservative Spiers criterion.

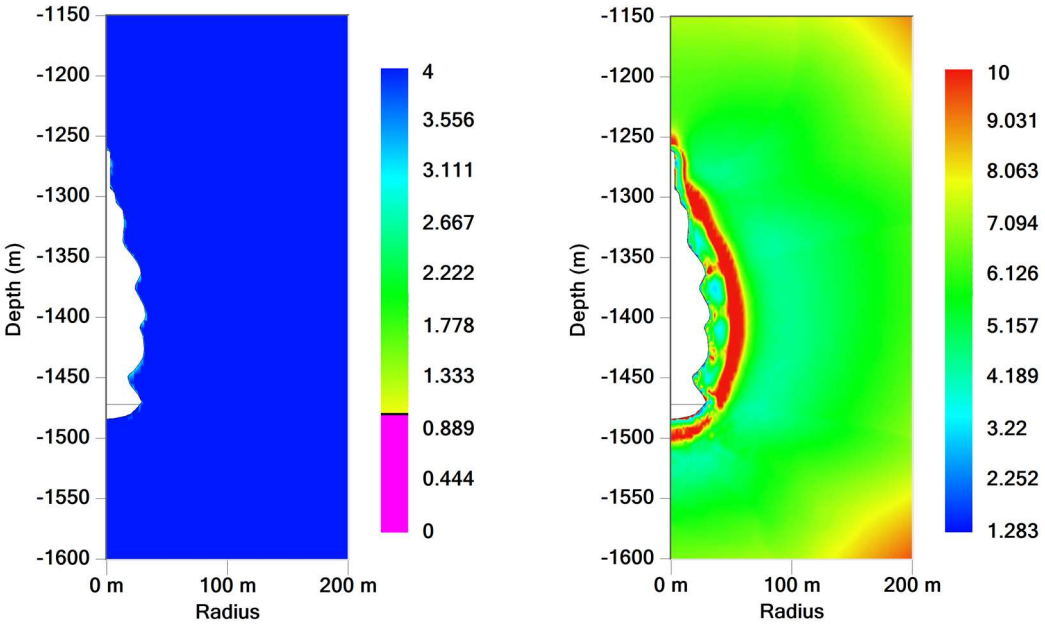

Fig. 9. Factor of safety (FoS) at the end of cyclic loading for Spiers (left) and DeVries (right) criteria.

Conclusion

This study provides a comprehensive numerical analysis of the mechanical stability of salt caverns for Underground Hydrogen Storage (UHS) under cyclic loading and rapid depressurization. The results demonstrate that cyclic operations induce significant creep closure and stress redistribution, leading to anisotropic deformation near the cavern walls, characterized by radial expansion and orthoradial contraction. Thermal stresses further exacerbate mechanical responses, highlighting the importance of temperature monitoring. The Factor of Safety (FoS) analysis, using both Spiers and DeVries criteria, confirms that the cavern remains structurally stable with no dilation zones detected, validating its integrity under the simulated conditions. However, the cumulative effects of cyclic loading on deformation and thermal behaviour emphasize the need for careful pressure cycling and gas velocities optimization and continuous monitoring of mechanical and thermal parameters to mitigate long-term risks. The findings contribute to a better understanding of salt cavern behaviour under operational solicitations and provide practical insights for the safe and efficient design of hydrogen storage.

Acknowledgments

This research was partly supported by funding from the Clean Hydrogen Partnership of the EU through the HyPSTER (n°101006751) and FrHyGe (n°101137892) projects.

References

Bérest P, Karimi-Jafari M, Brouard B (2007) Onset of tensile effective stresses in gas storage caverns. SMRI Fall Meeting, 119-135. https://hal.science/hal-00560262

Devries KL, Mellegard KD, Callahan GD, Goodman, WM (2005) Cavern roof stability for natural gas storage in bedded salty (850074, p 850074). https://doi.orh/10.2172/850074

Djizanne H, Brouard B, Hévin G (2023) Mechanical stability of a salt cavern used for hydrogen storage.15th ISRM Congress & 72nd Geomechanics Colloquium, Salzburg, Austria. Schubert & Kluckner, 2752–2757.

Munson DE, Dawson P (1982) Transient creep model for salt during stress loading and unloading. Tech. rep. SAND82-0962. Albuquerque, NM, USA: Sandia National Laboratories.

Spiers CJ, Peach CJ, Brzesowsky RH, Schutjens PM, Liezenberg JL, Zwart HJ (1988) Long term rheological and transport properties of dry and wet salt rocks. EUR 11848 prepared for Commission of European Communities, by University of Utrecht, Netherlands.